Journal of Solid State Chemistry **163,** 151–157 (2002)
doi:10.1006/jssc.2001.9386, available online at http://www.idealibrary.com on IDEAL®

Synthesis, Characterization, and Electrical Properties of the Series of Oxides $Ag_5Pb_{2-x}Cu_xO_6$ ($0.0 \leq x \leq 0.5$)

Eva M. Tejada-Rosales, Judith Oró-Solé, and Pedro Gómez-Romero[1]

Institut de Ciència de Materials de Barcelona (CSIC), Campus UAB, E-08193 Bellaterra, Barcelona, Spain

Received June 5, 2001; in revised form August 28, 2001; accepted August 30, 2001; published online November 27, 2001

The synthesis and characterization of a series of complex silver–lead–copper oxides is presented. These compounds constitute a solid solution with formula $Ag_5Pb_{2-x}Cu_xO_6$, ($0.0 \leq x \leq 0.5$), where Pb(IV) cations are substituted by Cu(II) cations. The synthesis was carried out by coprecipitation of Ag(I), Pb(II), and Cu(II) nitrates in alkaline media and made use of excess Ag(I) as a sacrificial reagent to oxidize lead to Pb(IV). The structure of the series is that of the parent $Ag_5Pb_2O_6$, with Cu(II) occupying part of the octahedral sites. This substitution induces interesting changes in the electric properties of the different members of the series, which range from metallic conductivity to semiconducting behavior. From Rietveld analysis for $Ag_5Pb_{1.5}Cu_{0.5}O_6$, the best fit is obtained for a model with Pb and Cu disordered over the octahedral site ($Ag_5Pb_{1.5}Cu_{0.5}O_6$, trigonal, $P\bar{3}1m$, $a = 5.8306(9)$ Å, $c = 6.3430(6)$ Å, $V = 187.37$ Å^3, $Z = 1$, $R_p = 7.16$, $R_{wp} = 9.26$, $R_{expected} = 5.88$, $R_{Bragg} = 3.94$, $\chi^2 = 2.48$).

Key Words: **silver–lead–copper oxides; solid solution; coprecipitation; Rietveld refinement; powder X-ray diffraction; electrical conductivity; conducting oxides.**

INTRODUCTION

Recently there have been many efforts to prepare complex silver–copper oxides in an attempt to synthesize new high-temperature superconductors similar to the mercury-containing phases that still hold record critical temperatures (1–3). These efforts aimed at the substitution of toxic mercury (4) by the chemically analogous and safer silver ions. In contrast with this interest, the chemistry of simple silver–copper oxides remained remarkably unexplored and it was not until very recently that the first known silver–copper oxide was reported (5–7). After this first success with the ternary compound $Ag_2Cu_2O_3$, we have continued our efforts to isolate new examples of other complex oxides in this system and present here the synthesis and characterization of what we believe are the first quaternary silver–copper oxides, specifically, a solid solution of formula $Ag_5Pb_{2-x}Cu_xO_6$, ($0.0 \leq x < 0.5$). There are important precedents to this family, although not containing both silver and copper, some of which have been central to its structural characterization. For instance, there are several copper–lead and silver–lead ternary oxides. There are two known copper–lead oxides, murdochite (Cu_6PbO_8) (8) and Cu_2PbO_2 (9), and also two silver–lead oxides, the metallic conductor $Ag_5Pb_2O_6$ (10–12) and Ag_2PbO_2 (10, 11, 13); the latter is isostructural with Cu_2PbO_2, whereas the former has been subject to studies with cation substitutions (In or Bi for Pb) (14) relevant to the present work.

As in the case of $Ag_2Cu_2O_3$, our approach in this work has centered on the use of low-temperature syntheses as an alternative to high-O_2-pressure methods in order to circumvent the relative low stability of the oxides sought and to avoid the formation of metallic silver.

EXPERIMENTAL SECTION

Synthesis

Powder samples of $Ag_5Pb_{2-x}Cu_xO_6$ were synthesized by coprecipitation of an aqueous solution containing $Cu(NO_3)_2 \cdot 3H_2O$ (Merck, p.a., 99.5%), $AgNO_3$ (Panreac, p.a., 99.98%), and $Pb(NO_3)_2$ (Fluka, 99%) in stoichiometric ratio. An excess of 3 moles of $AgNO_3$ per mole of product was added in the final optimized synthesis as an oxidizing agent. The necessary amounts of each salt for obtaining 0.3 g of $Ag_5Pb_{2-x}Cu_xO_6$ were dissolved in 4 mL of deionized water. The resulting solution was added to 6 mL of an aqueous solution of 3 M NaOH and a light brown precipitate formed, which could be aged and dehydrated by stirring in the solution for 4–8 hours, or by drying the solid at relatively low temperatures (90°C). After these treatments the precipitate turns into a black solid, which contains $Ag_5Pb_{2-x}Cu_xO_6$ and metallic silver. The precursor (before aging) or the final solid was vacuum filtered and washed with deionized water until the filtrate reached neutral pH. In both cases (aging at room temperature or mild heating) the

[1]To whom correspondence should be addressed. E-mail: pedro.gomez@icmab.es. Fax: + 34935805729.

0022-4596/02 $35.00

oxide was obtained quantitatively (according to its final weight).

Characterization

Atomic absorption analyses were carried out with a Unicam PU 9200X instrument for Cu, Ag, and Pb, using deuterium corrections. For thermal analyses a Perkin-Elemer TGA 7 was used. All the thermal experiments were carried out under a controlled dynamic atmosphere, heating at 2°C/min. For the determination of oxygen contents, an atmosphere of Ar/H_2 (5% vv H_2) was used. Microanalysis and electron diffraction were carried out using an analytical transmission electron microscope JEOL-JEM-1210. Microanalysis was performed on ca. 20 microcrystals for each sample. The powder X-ray data were collected in a Rigaku X-ray powder diffractometer "Rotaflex" Ru-200B, $10 < 2\theta < 70°$, step 0.02°, Cu$K\alpha$ radiation ($\lambda = 1.5418$ Å). X-ray diffraction data were used for the refinement of the crystal structure by the Rietveld method using the program FULLPROF (15). Four contact electrical conductivity measurements were made using a DC power apparatus (Keithley model 224) and a multimeter (Fluke model 8842A). The sample was prepared as cold-pressed pellets, using silver paste for contact. A CTI Cryogenics model 800 Cryo-Torr 100 cryostat and a LakeShore model DRC-91C controller were used for cooling and controlling the temperature. Magnetic susceptibility was measured under constant magnetic fields (10,000 G) in the temperature range 5–300 K by means of a Quantum Design SQUID magnetometer using approximately 20 mg of powdered sample.

RESULTS AND DISCUSSION

Room-Temperature Synthesis

The synthesis of the title oxide takes place by alkaline coprecipitation of a mixed solution of silver(I), lead(II), and copper(II) ions to yield an intermediate solid which, upon aging, leads to crystalline $Ag_5Pb_{2-x}Cu_xO_6$ in quantitative yield. This reaction is remarkable in that it represents a simple alternative to high-temperature, high-pressure procedures conventionally used to overcome the tendency of silver oxides and other noble transition-metal oxides toward thermal decomposition to yield the corresponding metals. As the oxidation state of lead in the final product is Pb(IV), an oxidizing agent is necessary. In the synthesis described here, Ag(I) acts as the oxidizing agent, thereby producing metallic silver as a consistent impurity. Two possible reaction schemes can be considered:

$$(9-2x)Ag^+ + (2-x)Pb^{2+} + xCu^{2+} + (13-2x)OH^- \rightarrow Ag_5(Pb_{2-x}Cu_x)O_{(13-2x)/2} + 2(2-x)Ag^0 + (13-2x)/2H_2O \quad [1]$$

or

$$8Ag^+ + (2-x)Pb^{2+} + xCu^{2+} + 12OH^- \rightarrow Ag_5(Pb_{2-x}Cu_x)O_6 + 3Ag^0 + 6H_2O. \quad [2]$$

Equation [1] implies the variation with x of the oxygen content in the final product, as well as variable amounts of metallic silver obtained depending on the copper content. The second possibility (Eq. [2]) implies constant oxygen and silver contents, independent of the copper content, x. In the second case the substitution of Cu(II) for Pb(IV) is compensated by a variation in the formal oxidation state of Ag. The undoped compound $Ag_5Pb_2O_6$ has silver in formal oxidation state of $Ag^{+0.8}$, while the last compound of the series, $Ag_5Pb_{1.5}Cu_{0.5}O_6$, has silver in oxidation state of Ag^+. TGA analyses (see below) show that the oxygen content of this series of compounds does not vary with the copper content; thus, the reaction that takes place is the second one, with a variation in the formal oxidation state of silver through the series.

Finally, it should be mentioned that, in order to avoid the presence of the necessary small impurities of metallic silver, several alternative oxidizing agents to Ag(I) were tried, though without much success, among them oxygen and hydrogen peroxide.

Chemical Analyses

Atomic absorption analyses of powder samples indicate the formula $Ag_8Pb_{2-x}Cu_xO_6$ for the bulk solid obtained, whereas quantitative EDX microanalyses indicate a composition consistent with the formula $Ag_5Pb_{2-x}Cu_xO_6$. Table 1 summarizes the results of the analyses of different samples by both methods. For the quantification of cation contents by EDX, $Ag_2Cu_2O_3$ and Ag_2PbO_2 were used as calibration standards (for Ag/Cu and Ag/Pb ratios). EDX analyses show the presence of Ag, Pb, and Cu in a constant ratio in the vast majority of the microcrystals analyzed for each different compound of the series, confirming the isolation of a pure homogeneous phase (as an explicit example,

TABLE 1
Results of Chemical and EDX Analyses for Several Synthetic Compositions

Nominal ratio			Stoichiometry by atomic absorption			Stoichiometry by EDX		
Ag	Pb	Cu	Ag	Pb	Cu	Ag	Pb	Cu
7.8	1.40	0.60	7.8	1.33	0.68	5	1.10	0.53
8.0	1.49	0.50	8	1.51	0.54	5	1.54	0.66
8.4	1.67	0.31	8.4	1.66	0.34	5	1.7	0.25
8.8	1.9	0.2	8.8	1.90	0.21	5	1.65	0.19

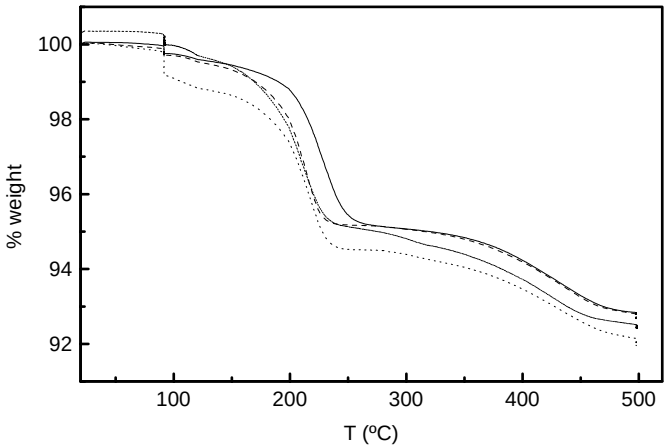

FIG. 1. Thermogravimetric analyses of $Ag_5Pb_{2-x}Cu_xO_6$ under Ar/H_2 dynamic atmospheres. Heating rate: 2°C/min. $x = 0$ (straight line), $x = 0.1$ (dashed), $x = 0.3$ (dot), $x = 0.5$ (segment). The sharp drop observed for each sample at 100°C is due to an isothermal step at that temperature.

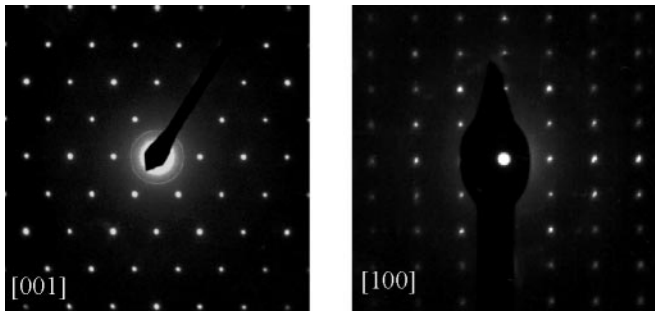

FIG. 2. Electron diffraction patterns for $Ag_5Pb_{1.5}Cu_{0.5}O_6$. The zone axes are indicated on each picture.

only 1 out of 17 microcrystals analyzed for a specific sample of $Ag_5Pb_{1.5}Cu_{0.5}O_6$ had a Ag/Pb/Cu ratio (very low Cu content in that case) statistically departing from average values). The oxygen content was determined by TGA in Ar/H_2 (5% vv). Figure 1 shows the thermal analysis of some of the compounds of the series $Ag_5Pb_{2-x}Cu_xO_6$ in Ar/H_2. TGA shows three different processes for the loss of weight with temperature: The first one corresponds to the loss of small amounts of loosely bound water. The second step takes place at ca. 200°C (note a significant difference in stability between the copper-free oxide ($x = 0$) and the others) and corresponds to the decomposition of the compound to give PbO, Ag, and Cu (determined by X-ray diffraction of the residue). Finally, the third step, with inflection points at ca. 425°C, corresponds to the loss of oxygen from PbO to give metallic lead. The percentages of weight loss are in agreement with this assignment and confirm that oxygen stoichiometry does not depend on copper content (x) and therefore confirms Eq. [2] above as the correct reaction scheme for the synthesis of these compounds.

Crystal Structure: Electron and Powder X-Ray Diffraction

Preliminary powder X-ray data showed diffraction patterns very similar to those of $Ag_5Pb_2O_6$, with a displacement of all the peaks to larger 2θ (smaller cell parameters) for $x > 0$. Electron diffraction studies allowed the reconstruction of the reciprocal lattice and established symmetry and the lack of systematic absences consistent with space group $P\bar{3}1m$. Figure 2 shows the electron diffraction patterns for the oxide $Ag_5Pb_{1.5}Cu_{0.5}O_6$ projected along [001] and [100].

Rietveld refinements were carried out for different compounds of the solid solution $Ag_5Pb_{2-x}Cu_xO_6$, using the structure of $Ag_5Pb_2O_6$ (10–12) as a starting structural model and considering several possibilities for the location of copper ions (initially both Ag sites and Pb sites were tried, but it soon became evident that the fit was better and the results more sound with Cu partially occupying the octahedral lead site). The occupancy of both Pb and Cu cations was finally refined with the only constraint of forcing their values to add to 2.00. The program used was FULLPROF (15). In successive cycles, atomic and profile parameters were refined, up to a total of 25, including isotropic displacement parameters for all atoms (copper and lead displacement parameters were refined together to avoid possible correlations with refined occupancy factors). The metallic silver impurity (3 moles of silver per mole of oxide according to Eq. [2]) was also considered in the refinement and treated as a second phase. Pseudo-Voigt functions were used to fit peak shapes between Lorentzian and Gaussian, and the peak width of the X-ray diffraction pattern was refined with the usual constraints (quadratic polynomial on $\tan\theta$) imposed by Caglioti's formula: $\mathrm{FWHM}^2 = U(\tan\theta)^2 + V\tan\theta + W$. Forty-nine peaks (3250 experimental points) were used in the refinement. The final refinement converged, yielding the reliability factors shown in Table 2. The experimental and calculated Rietveld profiles are shown in Fig. 3. It should be noted that the variation of peak width with θ suggests a sample peak broadening probably originating from a small grain size. We believe that this peak broadening, possibly anisotropic, is one of the factors responsible for the relatively large discrepancies

TABLE 2
Summary of Rietveld Results for $Ag_5Pb_{2-x}Cu_xO_6$

Sample	R_p	R_w	$R_{expected}$	R_{Bragg}	χ^2
$Ag_5Pb_2O_6$	10.0	13.2	9.10	5.56	2.11
$Ag_5Pb_{1.9}Cu_{0.1}O_6$	9.09	12.2	6.22	3.97	3.83
$Ag_5Pb_{1.5}Cu_{0.5}O_6$	7.16	9.26	5.88	3.94	2.48

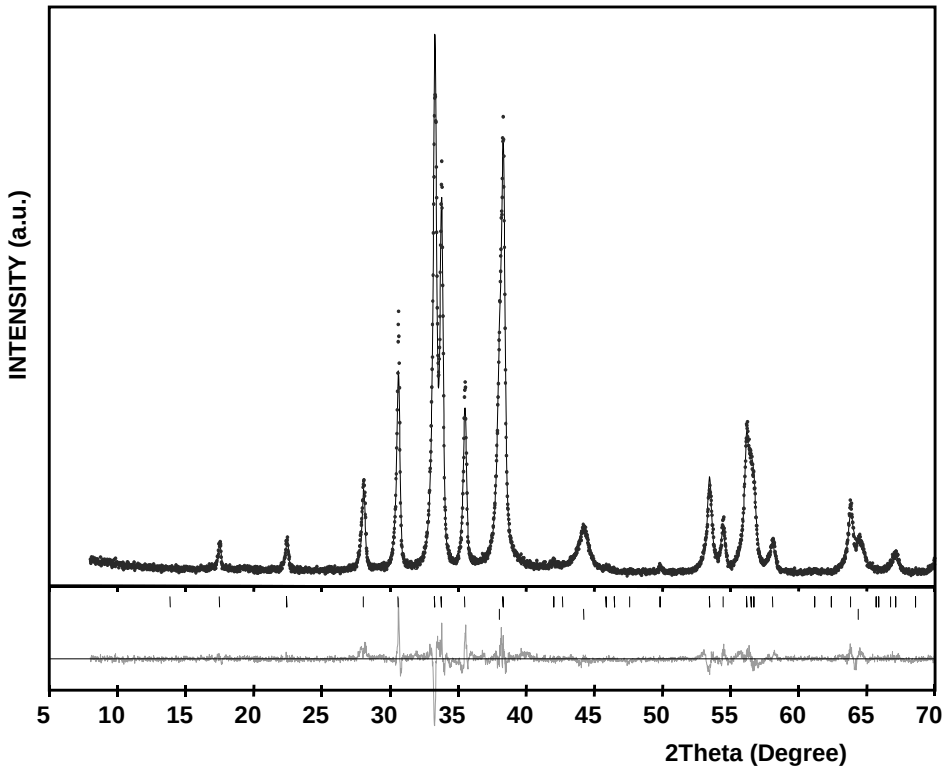

FIG. 3. Rietveld refinement for $Ag_5Pb_{1.5}Cu_{0.5}O_6$ structure. Dots correspond to experimental data, the continuous lines are the calculated profiles, and the bottom line shows the difference between the two. Small vertical lines mark the position of allowed Bragg reflections for $Ag_5Pb_{1.5}Cu_{0.5}O_6$ (top) and Ag (bottom).

in the observed and calculated intensities of several peaks.

The structure is shown in Fig. 4 and consists of layers formed by edge-sharing $(Pb,Cu)O_6$ octahedra alternating with three other layers of silver, sharing oxide anions with the octahedra. There are two symmetrically distinct silver atoms: Ag(2) with linear coordination, and Ag(1) with trigonal-pyramidal coordination (silver located at the vertex of a pyramid, the base of which is formed by three oxide ions). Oxide ions in turn (only one crystallographically independent) are tetrahedrally coordinated to one Ag(1), one Ag(2), and two (Pb,Cu) atoms. Table 3 shows fractional coordinates, isotropic displacement parameters for each atom, cell parameters, and peak shape parameters for the oxide $Ag_5Pb_{1.5}Cu_{0.5}O_6$. Table 4 summarizes relevant bond distances and angles for the same member of the solid solution. The cell parameters for other members are summarized in Table 5.

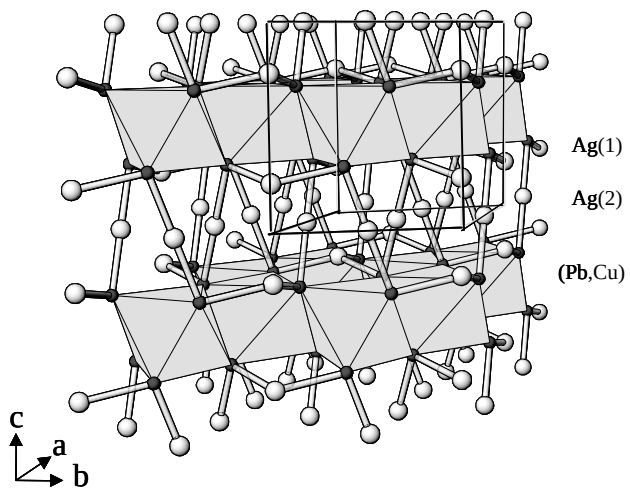

FIG. 4. Crystal structure of $Ag_5Pb_{2-x}Cu_xO_6$. Ag^{I} is shown as white spheres, Pb^{IV}/Cu^{II} as gray octahedra, and oxygen ions as small dark spheres. A unit cell is outlined.

We conclude that Cu(II) ions occupy the crystallographic positions of Pb(IV). The other possible metal substitutions were checked but none of them led to a satisfactory fit. It should be noted that the refined values for Pb/Cu occupancies (1.53(2)/0.4(2)) agree well with the expected ones for this compound (1.5/0.5). Furthermore, in the absence of any superstructure peaks, both in the powder X-ray pattern and, most significantly, in the electron diffraction patterns, we conclude a disordered arrangement of Cu and Pb in the octahedral sites as the best model consistent with

TABLE 3
Atomic Parameters (a) and Crystal and Refinement Parameters (b) Obtained by Rietveld Refinement for $Ag_5Pb_{1.5}Cu_{0.5}O_6$

Atom	x	y	z	B_{iso} (Å^2)	At./cell
(a)					
Ag1	0.000	0.000	0.2386(6)	5.4(1)	2
Ag2	0.500	0.000	0.000	3.9(1)	3
Pb	0.6667	0.3333	0.500	3.6(1)	1.53(2)
Cu	0.6667	0.3333	0.500	3.6(1)	0.47(2)
O	0.632(2)	0.0000	0.697(3)	1.4	6

Parameter	Refined value
(b)	
a	5.8306(9) Å
c	6.3430(6) Å
S	$0.755(7) \times 10^{-5}$
η_0	0.29(5)
U	0.53(3)
V	− 0.16391
W	0.099(4)
X	0.012(1)
zero	− 0.090(5)
Asy1	0.039(8)
Asy2	0.050(2)

our data. The paramagnetic behavior of the oxide $Ag_5Pb_{1.5}Cu_{0.5}O_6$ at high temperatures (1.7 Bohr magnetons per Cu ion) (Fig. 5), only affected by antiferromagnetic interactions at low temperature, is in agreement with this disorder.

TABLE 4
Selected Interatomic Distances (a) and Bond Angles (b) for $Ag_2Pb_{1.5}Cu_{0.5}O_6$

Atoms	Distance (Å)
(a)	
Ag(1)–O	$3 \times 2.18(1)$
Ag(2)–O	$2 \times 2.07(1)/3.25(1)$
Pb/Cu–O	$6 \times 2.23(1)$
Ag(1) ··· Ag(1)	3.027(5)/3.316(5)
Ag(1) ··· Ag(2)	3.285(2)
Ag(2) ··· Ag(2)	2.9135(4)
Pb/Cu ··· Pb/Cu	3.3649(6)/3.3670(3)

Atoms	Bond angle (°)
(b)	
O–Ag(1)–O	116.6(8)
Ag(1)–O–Ag(1)	47.2(4)/64.3(4) 70.2(6)/180(1)
O–Ag(2)–O	109.8(9)/69.8(3)/110.2(6) 47.6(5)/61.9(5)/36.4(2)
Ag(2)–O–Ag(2)	18.3(3)/47.3(3) 91.7(7)/82.2(8)/95.0(9)
O–Pb/Cu–O	171(1)
Pb/Cu–O–Pb/Cu	97.8(4)/28.9(3)/53.3(4)

TABLE 5
Refined Cell Parameters for Several Members of the Solid Solution $Ag_5Pb_{2-x}Cu_xO_6$

Sample	a (Å)	c (Å)	V (Å^3)
$Ag_5Pb_2O_6$	5.9326(14)[a]	6.4163(8)[a]	195.36[a]
$Ag_5Pb_{1.9}Cu_{0.1}O_6$	5.8899(10)	6.4116(6)	193.01
$Ag_5Pb_{1.5}Cu_{0.5}O_6$	5.8306(10)	6.3430(6)	187.37

[a] Compared to $a = 5.9324(3)$ Å, $c = 6.4105(4)$ Å, $V = 195.4$ Å^3 from Refs. (11) and (12).

Electrical Conductivity of $Ag_5Pb_{2-x}Cu_xO_6$

An electron count on the title series of oxides considering Pb(IV) and O(-II) leads to the formula $(Ag_5)^{4+}Pb_2^{4+}O_6^{2-}$ (for $x = 0$). This implies an electron in the 5*s* orbital of silver. As described previously, the crystal structure contains two types of silver atoms, Ag(2) with linear coordination typical of Ag(I) ions, and Ag(1), the latter forming a 3636 Kagomé substructure (16) with three Ag(1) atoms per unit cell. Interatomic Ag ··· Ag distances found in the silver–lead compound with no copper substitution are 3.093 and 3.317 Å between linear Ag(2) chains and 2.966 Å between Ag(1) in the Kagomé sublattice. For comparison, intermetallic distances in silver metal are 2.88 Å (14).

The electronic structure of $Ag_5Pb_2O_6$ has been extensively studied and discussed. Byström and Evers (10) suggested the presence of Ag–Ag bonds within silver chains, proposing a formula of the following type: $(Ag_2)^+Ag_3^+Pb_2^{4+}O_6^{2-}$. Based on conductivity measurements on the series $Ag_5Pb_{2-x}M(III)_xO_6$, Jansen *et al.* proposed the formulation (12, 14) $(Ag^+)_5Pb_2^{4+}O_6^{2-}(e^-)$, with a delocalized electron in the structure, which could explain the metallic character of the silver–lead compound. Based on calculations of the electronic structure, Brennan and Burdett (17) conclude that

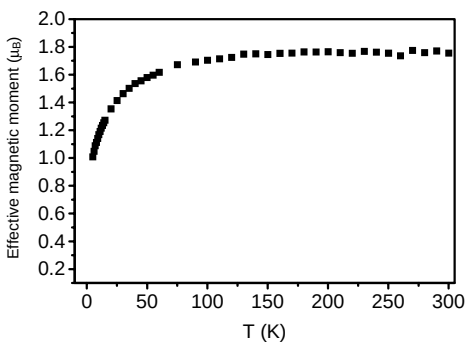

FIG. 5. Variation of the effective magnetic moment (per Cu atom) with temperature for $Ag_5Pb_{1.5}Cu_{0.5}O_6$.

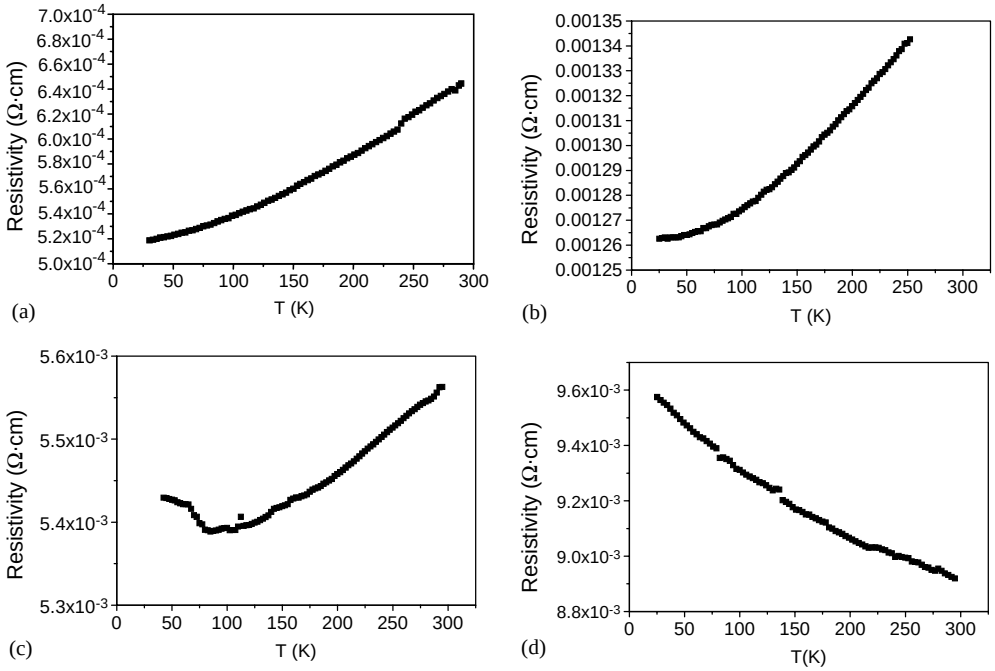

FIG. 6. Plot of resistivity vs temperature for (a) $Ag_5Pb_2O_6$, (b) $Ag_5Pb_{1.9}Cu_{0.1}O_6$, (c) $Ag_5Pb_{1.7}Cu_{0.3}O_6$, and (d) $Ag_5Pb_{1.5}Cu_{0.5}O_6$.

the unpaired electron is delocalized within the silver sublattice (including both Ag(1) and Ag(2)), thus proposing the formula $(Ag_5)^{4+}Pb_2^{4+}O_6^{2-}$. According to their calculations, the Fermi level cuts through a half-filled band with essentially silver *s* character (involving Ag(1) and Ag(2)).

The work by Bortz *et al.* doping $Ag_5Pb_2O_6$ by partial substitution of trivalent cations, Bi(III) or In(III), for Pb (IV) showed interesting results concerning both cell parameters and conductivity behavior (14). In that work, the authors reported the synthesis at temperatures close to 800°C and under high oxygen pressures of the series $Ag_5Pb_{2-x}M_xO_6$, ($0 \le x \le 1$ for $M =$ Bi, and $0 \le x \le 0.75$ for $M =$ In). Substitution of a small fraction of Bi(III) for Pb(IV) resulted in a drastic increase in resistivity. Thus, $Ag_5Pb_2O_6$ showed metallic behavior whereas the other end member of the solid solution, Ag_5PbBiO_6, was an insulator and, in between, other members showed semiconducting behavior. These qualitative changes were not observed in the case of the indium series. Substitution of In(III) for Pb(IV) led to a series of oxides with slightly increased resistivities as the amount of doping In(III) increased but always with metallic behavior.

In the title solid solution, substitution of Cu(II) for Pb(IV) is limited to values up to $x = 0.5$. But taking into account the stoichiometry and differences of charge, that value is equivalent to $x = 1.0$ for a substitution of any M(III) for Pb(IV), such as the Bi(III) and In(III) series reported by Bortz *et al.* (14). The substitution of copper for lead described here leads to a drastic change of electrical conductivity in these materials, similar to what was found for the family $Ag_5Pb_{2-x}Bi_xO_6$ (14), thus leaving the indium series as the anomalous case.

Indeed, the series $Ag_5Pb_{2-x}Cu_xO_6$ changes from metallic behavior for $x = 0$ (Fig. 6a) to semiconducting for $x = 0.5$ (Fig. 6d), while the values of resistivity grow drastically as the doping level increases. First, it should be noted that the presence of silver impurities in the samples does not compromise seriously the interpretation of conductivity properties, i.e., silver impurities do not reach a level sufficient for electronic percolation. This is demonstrated precisely by the change in electrical conductivity as the copper contents (but not silver impurities) changes from sample to sample. This behavior could be explained by considering either the number of carriers or the formal oxidation state of silver in each compound of the solid solution. Following Bortz and Jansen's notation, we can describe the undoped compound as $Ag_5^+Pb_2^{4+}O_6^{2-}$ (e^-); the compound with $x = 0.1$, as $Ag_5^+Pb_{1.9}^{4+}Cu_{0.1}^{2+}O_6^{2-}$ ($0.8e^-$), and, in general, the series should be formulated as $Ag_5^+Pb_{1.9}^{4+}Cu_{0.1}^{2+}O_6^{2-}((1-2x)e^-)$.

Finally, it should be mentioned that although there is a continuous transition between the metallic and semiconducting compositions, the intermediate members of the series show certain anomalies, in particular the oxide with $x = 0.3$, with a relative minimum in the curve of resistivity (Fig. 6c) which could deserve further attention and study from a physical point of view.

ACKNOWLEDGMENTS

This work was funded by CICYT (Spain) (MAT98-0807-C02-02, PB98-0491). We also thank the Ministry of Education and Culture (Spain) for a predoctoral fellowship awarded to E.M.T.-R.

REFERENCES

1. S. N. Putilin, E. V. Antipov, O. Chmaissem, and M. Marezio, *Nature* **362,** 226 (1993).
2. A. Tokiwa-Yamamoto, K. Isawa, M. Itoh, S. Adachi, and H. Yamauchi, *Physica C* **216,** 250 (1993).
3. J. L. Wagner, P. G. Radaelli, D. G. Hinks, J. D. Jorgensen, J. F. Mitchell, B. Dobrowski, G. S. Knapp, and M. A. Beno, *Physica C*: *Superconductivity* **210,** 447 (1993).
4. M. A. Alario-Franco, *Adv. Mater*. **7,** 229 (1995).
5. P. Gómez-Romero, E. M. Tejada-Rosales, and M. R. Palacín, *Angew. Chem*., *Int. Ed*. **38,** 524 (1999).
6. E. M. Tejada-Rosales, M. R. Palacín, and P. Gómez-Romero, *Boletín de la Sociedad Española de Cerámica y Vidrio* **39,** 209 (2000).
7. E. M. Tejada-Rosales, Ph.D. Thesis, Universitat Autònoma de Barcelona, Bellaterra, Barcelona, (2001).
8. C. L. Christ and J. R. Clark, *Am. Mineral*. **40,** 907 (1955).
9. H. Szillat and C. L. Teske, *Z. Anorg. Allg. Chem.* **620,** 1307 (1994).
10. A. Byström and L. Evers, *Acta Chem. Scand*. **4,** 613 (1950).
11. M. Jansen, M. Bortz, and K. Heidebrecht, *Z. Crystallogr*. **186,** 147 (1989).
12. M. Jansen, M. Bortz, and K. Heidebrecht, *J. Less-Common. Met*. **161,** 17 (1990).
13. M. Jansen and M. Bortz, *Z. Anorg. Allg. Chem.* **579,** 123 (1989).
14. M. Bortz, M. Jansen, H. Huhl, and E. Bucher, *J. Solid State Chem.* **103,** 447 (1993).
15. J. Rodriguez-Carvajal, Program FULLPROF, (1998).
16. A. F. Wells, "Three-Dimensional Nets and Polyhedra." Wiley, New York, 1977.
17. T. D. Brennan and J. K. Burdett, *Inorg. Chem.* **33,** 4794 (1994).